Ghost resonance in a semiconductor laser operating in an excitable regime

Claudio R. Mirasso[a], J.M. Buldú[b], Dante R. Chialvo[c,d], M.C. Torrent[b], and J. García-Ojalvo[b,e]

[a]Departament de Física, Universitat de les Illes Balears, E-07071 Palma de Mallorca, Spain
[b]Departament de Física i Enginyeria Nuclear, Universitat Politècnica de Catalunya, Colom 11, E-08222 Terrassa, Spain
[c]Department of Physiology, Northwestern University, Chicago, Illinois, 60611, USA
[d]Center for Studies in Physics and Biology, The Rockefeller University, New York, New York 10021, USA
[e]Center for Applied Mathematics, Cornell University, Ithaca NY 14583, USA

ABSTRACT

We show both numerically and experimentally that a semiconductor laser prepared in an excitable state and driven by two weak periodic signals with different frequencies is able to resonate at a *ghost* frequency, i.e., a frequency that it is not present in the forcing signal. The small signal modulation together with the complex internal dynamics of the system produces this resonance. This is an eminently nonlinear effect that agrees with the recent theoretical predictions by Chialvo et al. [Phys. Rev. E **65**, 050902(R), 2002].

1. INTRODUCTION

Semiconductor lasers subject to optical feedback have attracted the attention of the researchers for more than three decades. One of the most interesting regimes is the excitable regime. When the laser is biased close enough to threshold the system remains stable without any external perturbation. However, if a small modulation current is superimposed onto the bias current the system exhibits the three ingredients that are required in any excitable system: first, the existence of a threshold above which an excitation can occur; second, the form and size of the response is invariant to any change in the magnitude of the perturbation; third, a refractory time exists: if a second perturbation is applied at a time shorter than the refractory time, the system no longer responds.[1, 2]

For bias currents slightly higher these systems operates is the well known Low-Frequency Fluctuation regime (LFF) in which the output power of the laser suffers sudden dropouts to almost zero power at irregular time intervals when is biased close to threshold.[3] Although the LFF behavior has been observed already at the end of the seventies, its dynamics is not fully understood yet.

As already mentioned, recent experimental[1] and numerical[2, 4] reports show the conditions for which a laser subject to optical feedback and biased close to threshold is able to operate in an excitable regime, before the onset of the LFFs. It has been also shown both experimentally[5, 6] and numerically[7, 8] that a laser subject to optical feedback can also exhibit stochastic[9] and coherence[10] resonance when biased close to threshold, extending the richness of the dynamical behaviors of this system. While stochastic resonance is characterized by an optimum response of the system subject to a weak periodic signal for an intermediate value of the noise level, coherence resonance is characterized by an almost periodic response of the system to an intermediate level of noise but without any external periodic signal. Both effects have been also observed in a large variety of systems including periodic and chaotic systems.[9, 11]

Also recently it has been shown that the laser responses can be entrained to give a periodic train of dropouts by superimposing an external forcing to a bias current close to threshold. If the amplitude of the forcing is larger

---

than a certain value, the dropouts occur at the frequency of the external forcing when the latter has a frequency larger than the mean frequency of the dropouts in the absence of the perturbation.[12–14] More recently, it has been also shown that two laser coupled bidirectionally can exhibit a kind of power dropouts similar to the ones observed when the laser is subject to optical feedback.[15] Moreover, if one of these lasers is slightly modulated the power dropouts entrain to the modulation frequency much more efficiently than when one of the lasers is subject to optical feedback[16]

In all the previous studies, semiconductor lasers were excited at most with a *single* sinusoidal input. In this paper we go further and study numerically and experimentally the response of a semiconductor laser subject to optical feedback biased close to threshold and modulated by two weak sinusoidal signals. The main point of our results is that the system response shows a resonance at a frequency that is absent in the input signals. For this reason we call it *ghost* resonance. We describe the condition for and the location of this *ghost* resonant frequency which has been recently predicted, for a simpler system, by theoretical arguments.[17]

2. MODELLING AND SIMULATIONS

We are interested in the system response to modulation composed of multiple periodic signals $f_1, f_2, ...f_n$. Although the present work focus in the case of two components, the driving signal has the following general form:

$$I(t) = I_b \left\{1 + m \left[sin(2\pi(kf_0t + \Delta f\, t)) + sin(2\pi((k+1)f_0t + \Delta f\, t)) + ... + sin(2\pi((k+n-1)f_0t + \Delta f\, t))\right]\right\} \ , \ (1)$$

with $k > 1$ and n being the number of terms used. I_b is the bias current and m is the modulation amplitude. Here we choose to use the first two terms ($n = 2$) and f_0=4.5 MHz (although the same qualitative features would be observed for other choices of f_0). For simplicity, initially we describe results for $n = 2$ and $\Delta f = 0$, i.e., the singular case of harmonic signals.

The laser is modelled by the Lang-Kobayashi (L-K) model[18] that describes the dynamics of a semiconductor laser subject to weak/moderate optical feedback and accounts for single mode operation. It describes the time evolution of the slowly varying amplitude of the electric field E(t) and the excess carrier number N(t):

$$\frac{dE}{dt} = \frac{1 + i\alpha}{2}(G(E, N) - \gamma)\, E(t) + \kappa e^{-i\omega\tau}E(t - \tau) + \sqrt{2\beta N}\xi(t) \tag{2}$$

$$\frac{dN}{dt} = I_b(1 + m\{sin(2\pi(kf_0t + \Delta ft)) + sin(2\pi((k+1)f_0t + \Delta ft))\}) - \gamma_e\, N(t) - G(E, N)\, |E(t)|^2 \tag{3}$$

$$G(E, N) = \frac{g(N(t) - N_0)}{1 + s|E(t)|^2} \ . \tag{4}$$

The first term on the right hand side of Eq.(2) accounts for the stimulated emission. $\alpha = 3.4$ is the linewidth enhancement factor and $\gamma = 0.24$ ps^{-1} is the cavity decay rate. The second term is the feedback term which is described by two parameters: the feedback strength $\kappa = 20$ ns^{-1} and the external round–trip time $\tau = 5.57$ ns. $\omega/2\pi = 4.56 \times 10^{14}$ Hz is the laser free running frequency. The last term accounts for the spontaneous emission noise, considered as a Gaussian white noise source of zero mean and delta correlation, with a spontaneous emission rate $\beta = 5 \times 10^{-10}$ ps^{-1}. The first term in Eq.(3) accounts for the injection current with the two sinusoidal inputs at frequencies $2f_0$ and $3f_0$, being $f_0 = 4.5$ MHz and modulation amplitude m with respect to threshold. The second term accounts for the spontaneous recombination and the third one for the stimulated recombination. $I_b = 1.07\, I_{th}$ is the bias current, $I_{th} = 19.8$ mA is the threshold current and $\gamma_e = 0.62$ ns^{-1} is the carrier decay rate. Eq.(4) accounts for the material gain which depends on N and $|E|^2$. $N_0 = 1.5 \times 10^8$ is the number of carriers at transparency and $s = 1 \times 10^{-7}$ is the saturation gain coefficient.
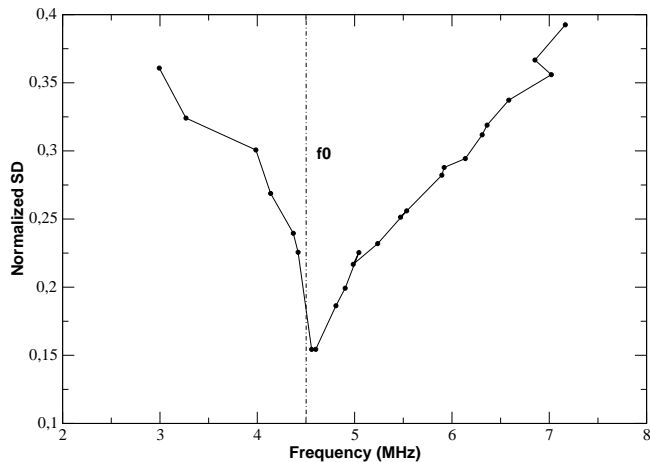
3. NUMERICAL RESULTS

In Fig. 1 we show examples of three representative time traces for low ($m = 0.005$), intermediate ($m = 0.012$) and high ($m = 0.028$) amplitude values of the injected signals obtained from the numerical integration of eqs. (2)-(4). It can be clearly seen that for the intermediate amplitude the dropouts are almost equally spaced at a time interval that corresponds grossly to $1/f_0$, a frequency that is not being injected. Thus the laser is detecting in a nonlinear way the subharmonic frequency. When computing the probability distribution function for a large number of dropouts we observe, for the optimum value of the amplitude, a clear peak at $1/f_0$ which indicates that the system is resonating with this frequency.
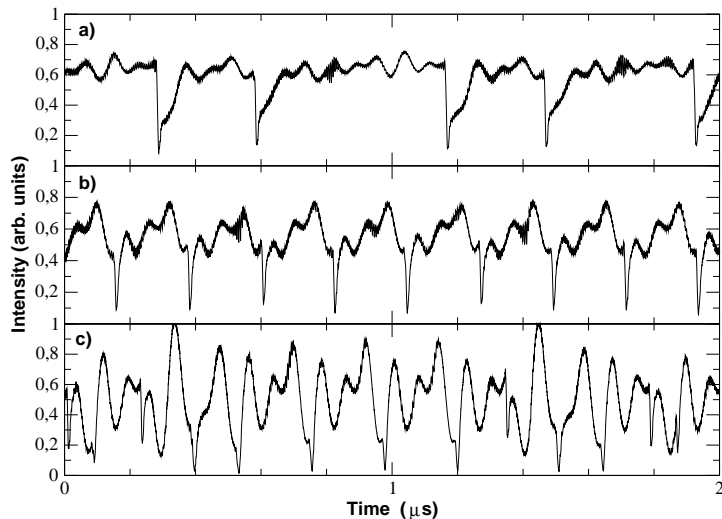
Figure 1: Numerical time series for low (a), intermediate (b) and high (c) amplitudes of the injected signals.

The resonance with the ghost frequency can be visualized by measuring the mean interval between dropout events and its standard deviation (SD) at various values of the signal amplitude m. Fig. 2 shows these results plotted as the normalized SD (i.e., SD/mean) as a function of the mean frequency of dropout events. It is clearly seen that the minimum is very close to f_0 (vertical dashed line), i.e., the ghost frequency.

Figure 2: Numerical results showing that the variability of the dropout intervals reaches a minimum for a frequency close to f_0.

The ghost frequency is not, as one naively would expect, simply the difference between the two components f_1 and f_2, (where $f_1 = 2f_0$ and $f_2 = 3f_0$). This is demonstrated by adding a small term (i.e., $\Delta f \neq 0$) which shifts equally both frequencies. In this case we observe that the resonant frequency shifts as well, despite the fact that the difference remains constant. Numerical results using $f_1 = 7$ to 10.5 MHz and $f_2 = 11.5$ to 15 MHz and selecting the optimum amplitude $m = 0.012$ are presented in Fig. 3. The format of the plot is meant to illustrate better the linear change of the resonant frequency f_R as a function of the frequency shift. The PDFs are plotted using frequency (i.e., inverse of the dropout intervals) axis and they are lined up with the f_1 frequency at which were obtained. It can be seen that the density of the most frequent dropouts lies on a straight line. The experimental results show a remarkable agreement with the theoretical prediction[17] defined by:

$$f_R = f_0 + \frac{\Delta f}{k + 0.5} \quad . \tag{5}$$
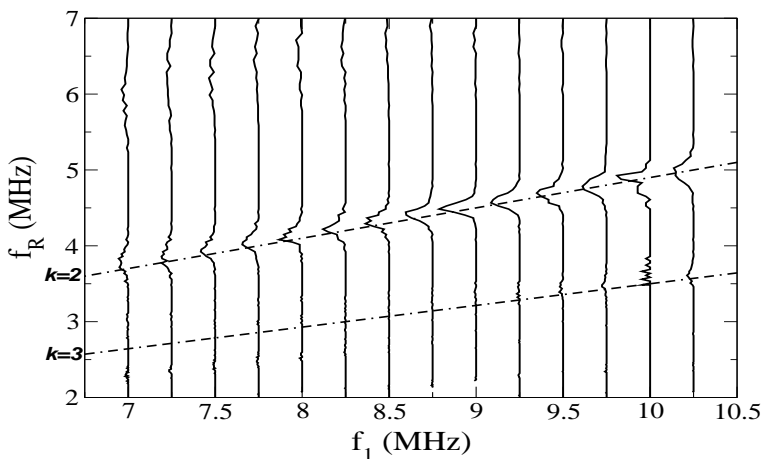
Figure 3: PDFs of the intervals between dropouts plotted as their inverse. For each pair of frequencies f_1-f_2 explored the PDF is plotted at the corresponding f_1 frequency. The lines are expected resonance frequencies from Eq.(5).

Since the range of f_1 we explored is about twice f_0, the dotted line labeled 'k=2' predicts the location of the most important resonance and the one 'k=3' the expected ones if the range where to be extended further up. Thus, the results presented in this figure agree very well with the ones described recently[17] for a simpler system.

4. EXPERIMENTAL RESULTS
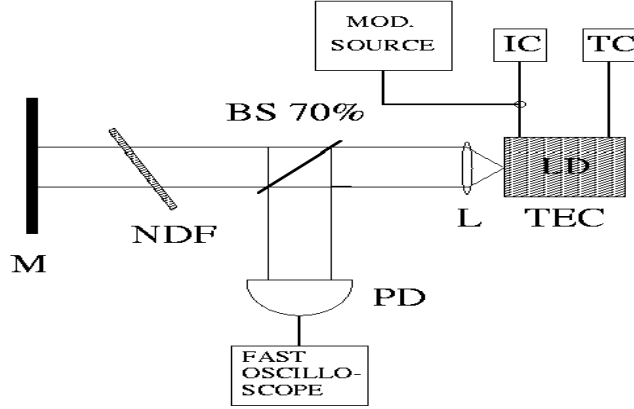
Figure 4: Experimental set-up.

In order to verify our numerical results we built up an experiment using a semiconductor laser subject to weak/moderate optical feedback and driven by two weak periodic signals. The experimental setup, shown in Fig. 4, consists of an index-guided AlGaInP semiconductor laser (Roithner RLT6505G), with a nominal wavelength of 658 nm. The threshold current is $I_{\mathrm{th}} = 18.4$ mA for a temperature of $19.86 \pm 0.01\,^{\circ}$C. The injection current (IC), without modulation, is set to 19.7 ± 0.1 mA all through the experiment. An antireflection-coated laser-diode objective (L) is used to collimate the emitted light. An external mirror (M) is placed 83.5 cm away from the front facet of the laser, introducing a delay time of $\tau \sim 5.56$ ns. The feedback strength is such that it yields a threshold reduction of 7.0% and it is adjusted by placing a neutral density filter (NDF) in the external cavity. The output intensity is collected by a fast photodetector (PD) and analyzed with a 500 MHz bandwidth acquisition card.
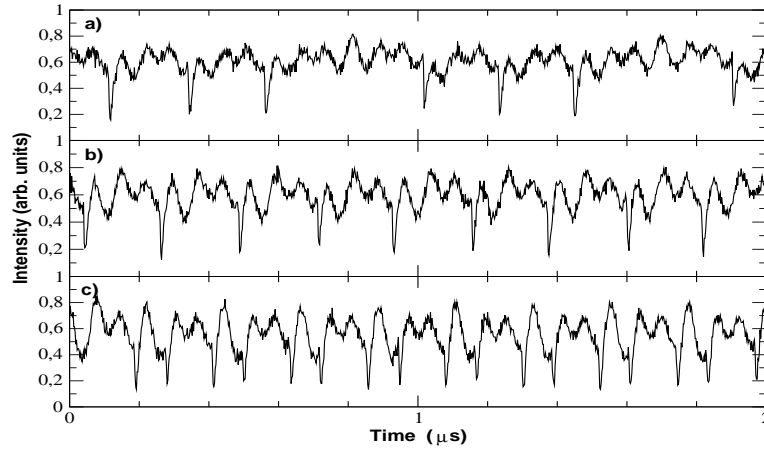

Figure 5: Experimental time series for low (a), medium (b) and high (c) injected signals.

In Fig. 5 we show examples of three representative time traces for low ($m = 0.057$), intermediate ($m = 0.0815$) and high ($m = 0.114$) amplitude values of the injected signals. It can be clearly seen that for the intermediate amplitude the dropouts are almost equally spaced at a time interval that corresponds grossly to $1/f_0$, a frequency that is not being injected. As explained before, the laser is detecting in a nonlinear way the subharmonic frequency.
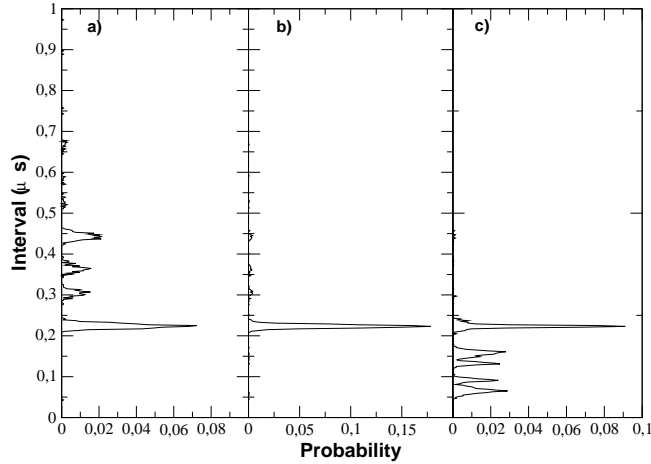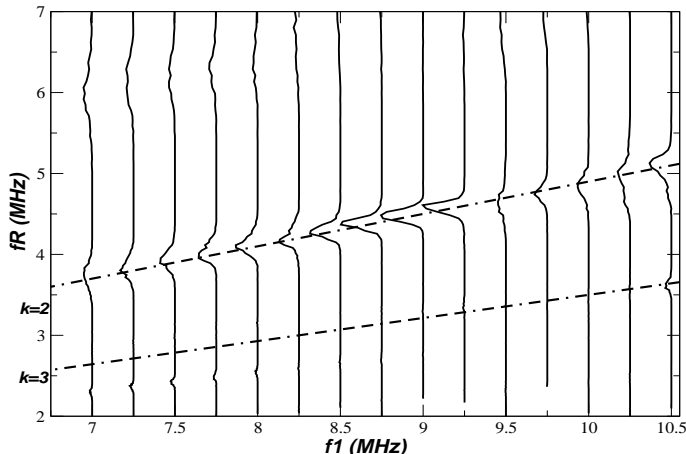
Figure 6: Experimental PDFs of the dropouts intervals at the three amplitudes, low (a), intermediate (b) and high (c) injected signals. The PDFs largest peak corresponds to $1/f_0$.

To better visualize this fact we plot on figure 6 the probability distribution functions (PDF) for a large number of dropouts (approx. 1500). For the small amplitude (panel a) it can be observed a peak at a time $1/f_0$ other peaks at longer times which indicate that the system responds sometimes to f_0 although at some others times dropouts are skipped. For the optimum value of the amplitude (panel b) the PDF has a clear peak at $1/f_0$ which indicates that the system is resonating with this frequency. For the higher amplitude (panel c) there are several peaks at different times corresponding to higher frequencies.
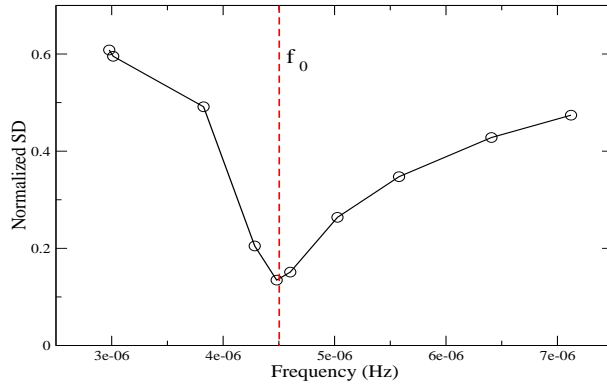
Figure 7: Experimental results showing that the variability of the dropout intervals reaches a minimum when its frequency approaches f_0.

Fig. 7 shows the results of the normalized SD (i.e., SD/mean) as a function of the mean frequency of dropout events. It is clearly seen that the minimum is very close to f_0 (vertical dashed line), i.e., the ghost frequency, in agreement with the numerical predictions.

Figure 8: Experimental results. PDFs of the intervals between dropouts are plotted as in fig. 4. The lines are expected resonance frequencies from Eq.(5).

We have also added to the signals forcing a small term (i.e., $\Delta f \neq 0$) which shifts equally both frequencies, as we have done numerically. In this case we observe that the resonant frequency shifts as well, despite the fact that the difference remains constant, in a very good agreement with the numerical predictions. Results from experimental runs using $f_1 = 7$ to 10.5 MHz and $f_2 = 11.5$ to 15 MHz and selecting the optimum amplitude $m = 0.0815$ are presented in Fig. 8. As previously, the format of the plot is meant to illustrate better the linear change of the resonant frequency f_R as a function of the frequency shift. The PDFs are plotted using frequency (i.e., inverse of the dropout intervals) axis and they are lined up with the f_1 frequency at which were obtained. It can be seen that the density of the most frequent dropouts lies on a straight line. The experimental results also show a remarkable agreement with the theoretical prediction[17] and defined by Eq. (5).

Again, since the range of f_1 we explored is about twice f_0, the dotted line labeled 'k=2' predicts the location of the most important resonance and the one 'k=3' the expected ones if the range where to be extended further up. Thus, the results presented in this figure agree extremely well with the ones described previously in a simpler system[17] and it is an experimental demonstration of this type of resonance at the ghost frequency.

Under the current experimental conditions is cumbersome to change the noise intensity, and thus one is unable to fully explore the stochastic aspects of this resonance as was done in.[17] We find that the most robust results are obtained when the bias is tuned close to the threshold for LFF, a region where the effects of even minute fluctuations are expected to be magnified. The origin of these fluctuations, whether they are induced by the internal nonlinear dynamics or by stochastic sources remains unclear. The consequences of these aspects deserve to be explored in future work.

5. CONCLUSIONS

In conclusion, we have described, both numerically experimentally a new type of resonance observed when a semiconductor laser subject to optical feedback is biased close to its excitable dynamics, near the onset of the low-frequency fluctuation regime. It is shown that when this system is modulated with two weak periodic signals of different frequencies exhibits a resonance at a *ghost* frequency, i.e., a frequency that it is not present in the modulating input. We find that for injection frequencies kf_0 and $(k + 1)f_0$, being f_0 any slow frequency, we observe the resonance at exactly f_0, a frequency that is not present in the injection current. It is also observed that when a constant shift is added to both frequencies of the injected signal the resonance does not appear at the difference between the two frequencies but at a frequency that follows a simple linear relationship. Our results confirm the recent theoretical predictions by Chialvo and coworkers, based on a more simpler system.[17]

ACKNOWLEDGEMENT

REFERENCES

1. M. Giudici, C. Green, G. Giaconelli, U. Nespolo, and J. R. Tredicce, "Andronov bifurcation and excitability in semiconductor lasers with optical feedback," *Phys. Rev. E* **55**, pp. 6414–6418, 1997.
2. J. Mulet and C. R. Mirasso, "Numerical statistics of power dropouts based on the lang-kobayashi model," *Phys. Rev. E* **59**, pp. 5400–5405, 1999.
3. C. Risch and C. Voumard, "Self-pulsation in the output intensity and spectrum of gaas-algaas cw diode lasers coupled to a frequency-selective external optical cavity," *J. Appl. Phys.* **58**, pp. 2083–2085, 1977.
4. M. C. Eguía, G. Mindlin, and M. Giudici, "Low-frequency fluctuations in semiconductor lasers with optical feedback are induced with noise," *Phys. Rev. E* **58**, pp. 2636–2639, 1998.
5. G. Giacomelli, M. Giudici, S. Balle, and J. R. Tredicce, "Experimental evidence of coherence resonance in an optical system," *Phys. Rev. Lett.* **84**, pp. 3298–3301, 2000.
6. F. Marino, M. Giudici, S. Barland, and S. Balle, "Experimental evidence of stochastic resonance in an excitable optical system," *Phys. Rev. Lett.* **88**, pp. 040601–040604, 2002.
7. J. M. Buldú, J. García-Ojalvo, C. R. Mirasso, M. C. Torrent, and J. Sancho, "Effect of external noise correlation in optical coherence resonance," *Phys. Rev. E* **64**, pp. 051109–051112, 2001.
8. J. M. Buldú, J. García-Ojalvo, C. R. Mirasso, and M. C. Torrent, "Stochastic entrainment of optical power dropouts," *Phys. Rev. E* **66**, pp. 021106–021110, 2002.
9. L. Gammaitoni, P. Hanggi, P. Jung, and F. Marchesoni, "Stochastic resonance," *Rev. Mod. Phys.* **70**, pp. 223–287, 1998.
10. A. Pikovsky and J. Kurths, "Coherence resonance in a noise-driven excitable system," *Phys. Rev. Lett.* **78**, pp. 775–778, 1978.
11. C. Palenzuela, R. Toral, C. R. Mirasso, O. Calvo, and J. Gunton, "Coherence resonance in chaotic systems," *Europhys. Lett.* **56**, pp. 347–353, 2001.
12. J. Mulet, *Statistics of power dropouts in semiconductor lasers with optical feedback*, Master Thesis, Universitat de les Illes Balears, Palma de Mallorca, Spain, 1998.
13. D. W. Sukow and D. J. Gauthier, "Entraining power-dropout events in an external-cavity semiconductor laser using weak modulation of the injection current," *IEEE J. of Quantum Electron.* **36**, pp. 175–183, 2000.
14. J. M. Mendez, R. Laje, M. Giudici, J. Aliaga, and G. B. Mindlin, "Dynamics of periodically forced semiconductor laser with optical feedback," *Phys. Rev. E* **63**, pp. 066218–066223, 2001.
15. T. Heil, I. Fischer, W. E. asser, J. Mulet, and C. R. Mirasso, "Chaos synchronization and spontaneous symmetry-breaking in symmetrically delay-coupled semiconductor lasers," *Phys. Rev. Lett.* **86**, pp. 795–798, 2001.
16. J. M. Buldu, R. Vicente, T. Perez, C. R. Mirasso, M. C. Torrent, and J. Garcia-Ojalvo, "Periodic entrainment of power dropouts in mutually coupled semiconductor lasers," *Appl. Phys. Lett.* **81**, pp. 5105–5107, 2002.
17. D. R. Chialvo, O. Calvo, D. L. Gonzalez, O. Piro, and G. V. Savino, "Subharmonic stochastic synchronization and resonance in neuronal systems," *Phys. Rev. E* **65**, pp. 050902(R)–050905(R), 2002.
18. R. Lang and K. Kobayashi, "External optical feedback effects on semiconductor injection laser properties," *IEEE J. of Quantum Electron.* **16**, pp. 347–355, 1980.